AIMS Mathematics, 10(8): 19126–19146.
DOI: 10.3934/math.2025855
Received: 07 June 2025
Revised: 09 August 2025
Accepted: 19 August 2025
Published: 22 August 2025

http://www.aimspress.com/journal/Math

Research article

Analysis of a Brusselator reaction-diffusion model with nonlinear inhibition

Shouzong Liu*, **Yaxin Niu and Peiyang Chai**

College of Mathematics and Statistics, Xinyang Normal University, Xinyang 464000, China

* **Correspondence:** Email: liushouzong@163.com.

Abstract: In this paper, the pattern formation of a Brusselator reaction-diffusion model with nonlinear inhibition was investigated. Through linear stability analysis and spectral theory, mathematical criteria for the existence and stability of spatial patterns were established. The main results included explicit stability conditions for homogeneous steady states and spectral criteria linking eigenvalue multiplicities to pattern existence. A series of numerical simulations were performed to validate theoretical predictions, revealing clear transitions between uniform and spatially heterogeneous solutions. The work provides fundamental insights into pattern-forming mechanisms for controlling spatial organization in nonlinear reaction-diffusion systems.

Keywords: Brusselator model; reaction-diffusion equations; steady-state solution; stability; pattern formation
Mathematics Subject Classification: 35J25, 35K50, 47H11, 58C15

1. Introduction

Chemical oscillations and spatiotemporal pattern formation are among the most fascinating phenomena in nonlinear science, widely observed in biological, chemical, and ecological systems [1, 2]. A classical example of such behavior is found in autocatalytic reaction systems, where intermediate products can catalyze their own formation [3]. Among these, the Brusselator model proposed by Prigogine and Lefever has served as a prototypical model for studying chemical oscillations and spatial pattern formation [4]. It captures the essential dynamics of autocatalytic reactions with simple reaction kinetics and has been extensively employed to study self-organization in chemical and biological contexts [5–7].

The Brusselator model typically consists of two components, denoted $m(x,t)$ and $n(x,t)$, representing the concentrations of reactants or intermediates in the reaction [8]. In its simplest form, the Brusselator model includes two key reaction pathways [9]: One for the autocatalytic production of m, driven by interactions between m and n, leading to self-amplification; and one for the replenishment

mechanism of n, sustained by the reactant influx and selectively consumed in the autocatalytic cycle. These reactions are usually governed by the following system of partial differential equations (PDEs), which include both the reaction terms and diffusion terms:

$$\begin{cases} \dfrac{\partial m}{\partial t} = D_m \Delta m + f(m,n), \\ \dfrac{\partial n}{\partial t} = D_n \Delta n + g(m,n), \end{cases} \tag{1.1}$$

where D_m and D_n are the diffusion coefficients of m and n, respectively, $f(m,n)$ and $g(m,n)$ represent the nonlinear reaction terms that describe the chemical interactions, and Δ is the Laplace operator that accounts for spatial diffusion. The simplest form of the reactions $f(m,n)$ and $g(m,n)$ are typically given by

$$f(m,n) = a - (b+1)m + cm^2 n, \quad g(m,n) = bm - cm^2 n,$$

where $a > 0$ and $b > 0$ are constant reactant concentrations, and $c > 0$ denotes the autocatalytic rate constant. The nonlinearity $cm^2 n$ in the reaction terms drives the system's bifurcation behavior, enabling transitions between stable steady states and oscillatory regimes [10–13].

While the above simple Brusselator model has provided significant insights into nonlinear chemical dynamics, its biological relevance is limited by the assumption of unbounded autocatalytic growth. To address this limitation, we propose a modified formulation incorporating nonlinear inhibition effects. Specifically, we replace the standard autocatalysis term $cm^2 n$ with a resource-limited autocatalytic term $\frac{cm^2 n}{1+m}$, which introduces a nonlinear inhibition mechanism to the autocatalysis [14–16].

Beyond specialized applications, the original model's absence of resource constraints limits its application across dynamic systems involving competitive interactions. For example, in microbial metabolic networks where substrate availability governs reaction kinetics, the unmodified framework cannot capture essential feedback regulation. Our resource-limited formulation provides a quantitative tool for modeling such interactions, enabling improved predictions for industrial bioprocess optimization and extending the model's relevance to diverse applied sciences.

Mathematically, replacing $cm^2 n$ with $\frac{cm^2 n}{1+m}$ introduces a crucial saturation-modified mechanism. When m becomes large, the modified term's dependence on m transitions from quadratic order (m^2) to linear order (m), significantly slowing autocatalytic amplification compared to the original term. This mathematical property reflects biological systems where reaction rates are constrained by resource limitations and enzyme saturation, while maintaining behavioral continuity near $m = 0$ where the modified term approximates the original model.

In addition, to enhance biological plausibility, we will adopt initial and boundary value conditions, following earlier work on Brusselator-type systems [17] and their subsequent extensions [18, 19], to analyze the systems dynamics under physiologically relevant constraints. Specifically, we consider the system evolution on a bounded spatial domain $\Omega \subseteq \mathbb{R}^d$ ($d \geq 1$) over a time interval $[0, T)$, subject to the following conditions:

$$m(x,0) = m_0(x) > 0, \quad n(x,0) = n_0(x) > 0, \quad \forall x \in \overline{\Omega}, \tag{1.2}$$

$$\frac{\partial m}{\partial \nu} = \frac{\partial n}{\partial \nu} = 0, \quad (x,t) \in \partial\Omega \times (0,T), \tag{1.3}$$

where $m_0(x)$ and $n_0(x)$ represent continuous functions in $\overline{\Omega}$, and ν denotes the outward normal vector to the domain boundary. These conditions ensure mass conservation within the closed system. The

homogeneous Neumann (zero-flux) boundary conditions $\frac{\partial m}{\partial \nu} = 0$, $\frac{\partial n}{\partial \nu} = 0$ reflect a closed/semi-closed system, where reactants in domain Ω are conserved. Such systems are typical of intracellular compartments or confined biological regions (sites of frequent autocatalytic reactions). This contrasts with Dirichlet conditions, which model open systems with external reservoirs/sinks and can fundamentally alter the central self-organizing dynamics of pattern formation in this model [20–22]. To enhance biological relevance regarding initial states, non-uniform initial conditions $m_0(x)$ and $n_0(x)$ representing spatial heterogeneity are employed in our study.

Then the resulting complete initial-boundary value problem is formulated as

$$\begin{cases} \dfrac{\partial m}{\partial t} = D_m \Delta m + a - (b+1)m + \dfrac{cm^2 n}{1+m}, & (x,t) \in \Omega \times (0,T), \\ \dfrac{\partial n}{\partial t} = D_n \Delta n + bm - \dfrac{cm^2 n}{1+m}, & (x,t) \in \Omega \times (0,T), \\ m(x,0) = m_0(x), \quad n(x,0) = n_0(x), & x \in \Omega, \\ \dfrac{\partial m}{\partial \nu} = \dfrac{\partial n}{\partial \nu} = 0, & (x,t) \in \partial\Omega \times (0,T). \end{cases} \tag{1.4}$$

The primary objective of this work is to conduct a comprehensive analysis of the qualitative behavior of system (1.4), including the global existence and boundedness of classical solutions, the linear stability thresholds of homogeneous steady states, as well as the criteria for Turing-type bifurcations that govern the emergence of spatially heterogeneous patterns under nonlinear inhibition mechanisms.

The paper is organized as follows. In Section 2, we present the main theoretical results concerning solution properties, stability analysis, and pattern formation criteria. Section 3 provides numerical simulations that validate the theoretical predictions across various parameter regimes. Finally, Section 4 presents a brief conclusion.

2. Main results

2.1. Existence of global solutions

First, we establish the positivity of solutions of system (1.4).

Proposition 1. *Let $(m(x,t), n(x,t))$ be a classical solution of system (1.4) in $\Omega \times [0, T_{\max})$, where $T_{\max}$ denotes the maximal existence time of the solution, and then $m(x,t) > 0$ and $n(x,t) > 0$ for all $(x,t) \in \Omega \times [0, T_{\max})$.*

Proof. We prove the positivity of $m(x,t)$ and $n(x,t)$ by contradiction, using the strong maximum principle for parabolic equations.

Assume for contradiction that there exists $t \in (0, T_{\max})$ and $x \in \Omega$ such that $m(x,t) \le 0$. Define the first such time as

$$t_0 = \inf \left\{ t \ge 0 \,\middle|\, \exists x \in \Omega,\ m(x,t) \le 0 \right\}.$$

The assumption $m_0(x) > 0$ ensures $t_0 > 0$. At (x_0, t_0), where $m(x_0, t_0) = 0$ (the global minimum over $\overline{\Omega} \times [0, t_0]$), the strong maximum principle and homogeneous Neumann boundary conditions imply $\partial_t m(x_0, t_0) \le 0$ and $\Delta m(x_0, t_0) \ge 0$ (if $x_0 \in \Omega$) or $\Delta m(x_0, t_0) \ge 0$ in the viscosity sense (if $x_0 \in \partial\Omega$).

Substituting $m(x_0, t_0) = 0$ into the first equation of (1.4), we obtain

$$\partial_t m(x_0, t_0) = D_m \Delta m(x_0, t_0) + a - (b+1)m(x_0, t_0) + \frac{cm(x_0, t_0)^2 n(x_0, t_0)}{1 + m(x_0, t_0)}.$$

By simplifying with $m(x_0, t_0) = 0$ and $\Delta m(x_0, t_0) \geq 0$, we get $\partial_t m(x_0, t_0) = D_m \Delta m(x_0, t_0) + a > 0$. This contradicts $\partial_t m(x_0, t_0) \leq 0$. Hence, $m(x, t) > 0$ for all $(x, t) \in \Omega \times [0, T_{\max})$.

Similarly, assume that there exists $t \in (0, T_{\max})$ and $x \in \Omega$ such that $n(x, t) \leq 0$ and define

$$t_1 = \inf \left\{ t \geq 0 \,\middle|\, \exists x \in \Omega,\ n(x, t) \leq 0 \right\}.$$

We have $t_1 > 0$, and at $t = t_1$, there must exist $x_1 \in \Omega$ such that $n(x_1, t_1) = 0$, $\Delta n(x_1, t_1) \geq 0$, and $\partial_t n(x_1, t_1) \leq 0$.

Substituting $n(x_1, t_1) = 0$ into the second equation of (1.4), we get

$$\partial_t n(x_1, t_1) = D_n \Delta n(x_1, t_1) + bm(x_1, t_1) \geq bm(x_1, t_1) > 0,$$

which contradicts $\partial_t n(x_1, t_1) \leq 0$. Therefore, $n(x, t) > 0$ for all $(x, t) \in \Omega \times [0, T_{\max})$. The proof is complete. □

Theorem 1. *Let $D_m = D_n = D > 0$, and then system (1.4) admits a unique global classical solution $(m(x, t), n(x, t))$ with $m(x, t) > 0$ and $n(x, t) > 0$ for all $(x, t) \in \overline{\Omega} \times [0, \infty)$.*

Proof. By the classical existence theory for parabolic equations, system (1.4) admits a unique classical solution $((m(x, t), n(x, t))$ defined on a maximal interval $[0, T_{\max})$. To prove the global existence, we demonstrate $T_{\max} = \infty$ via uniform L^∞-bounds for $m(x, t)$ and $n(x, t)$.

First, we consider the lower bound for $m(x, t)$. Define $m_{\min}(t) = \min_{x \in \overline{\Omega}} m(x, t)$. Under Neumann boundary conditions, the minimum of m is either attained in the interior of Ω or on $\partial\Omega$. If the minimum occurs at a interior point, obviously, the Laplacian satisfies $\Delta m \geq 0$ at this point. If the minimum occurs at a boundary point, the boundary condition $\partial_\nu m = 0$ implies that the spatial derivatives vanish, and the Laplacian satisfies $\Delta m \geq 0$ at that point. From the first equation of system (1.4),

$$\partial_t m \geq a - (b + 1)m$$

holds at the spatial minimum point. Solving the differential inequality

$$\frac{d}{dt} m_{\min} \geq a - (b + 1)m_{\min}$$

with $m_{\min}(0) \geq \min_{\overline{\Omega}} m_0(x) > 0$, we obtain

$$m_{\min}(t) \geq \frac{a}{b + 1} + \left(m_{\min}(0) - \frac{a}{b + 1} \right) e^{-(b+1)t}.$$

Since $\lim_{t \to \infty} m_{\min}(t) \geq \frac{a}{b+1} > 0$, there exists a constant $m^l = \min \left\{ \frac{a}{2(b+1)}, \min_{\overline{\Omega}} m_0(x) \right\} > 0$ such that

$$m(x, t) \geq m^l \quad \text{for all } (x, t) \in \overline{\Omega} \times [0, T_{\max}).$$

Next, we further determine the upper bound for $n(x, t)$. Select $m_1 \in (0, m^l)$ sufficiently small such that

$$\frac{b(1 + m_1)}{cm_1} \geq \max_{x \in \overline{\Omega}} n_0(x).$$

Let $n_{\max}(t) = \max_{x\in\overline{\Omega}} n(x,t)$. At the spatial maximum point, $\Delta n \le 0$, and the second equation of system (1.4) yields

$$\partial_t n \le \frac{cm^2}{1+m}\left(\frac{b(1+m_1)}{cm_1} - n\right).$$

If $n_{\max}(t) > \frac{b(1+m_1)}{cm_1}$, then the right-hand side becomes negative, forcing $n_{\max}(t)$ to decay. By the maximum principle, we deduce

$$n(x,t) \le \frac{b(1+m_1)}{cm_1} \quad \text{for all } (x,t) \in \overline{\Omega}\times[0,T_{\max}).$$

Adding the first two equations of system (1.4), we get

$$\partial_t(m+n) = D\Delta(m+n) + a - m.$$

By rewriting, we deduce

$$\partial_t(m+n) - D\Delta(m+n) + (m+n) = a + n.$$

Using the lower bound $m \ge m_1 > 0$ and the upper bound $n \le \frac{b(1+m_1)}{cm_1}$, we have

$$\partial_t(m+n) - D\Delta(m+n) + (m+n) \le a + \frac{b(1+m_1)}{cm_1}.$$

Let $C_0 = a + \frac{b(1+m_1)}{cm_1}$. Applying the maximum principle to $w(x,t) = m(x,t) + n(x,t)$, we obtain

$$w(x,t) \le \max\left\{C_0, \max_{x\in\overline{\Omega}}(m_0(x) + n_0(x))\right\} \quad \text{for all } (x,t) \in \overline{\Omega}\times[0,T_{\max}).$$

Thus, $m(x,t)$ and $n(x,t)$ are uniformly bounded above.

Since $m(x,t)$ and $n(x,t)$ are uniformly bounded in $L^\infty(\Omega)$ on $[0,T_{\max})$, standard parabolic regularity theory implies that $T_{\max} = \infty$. Therefore, the solution exists globally. The proof is complete. □

Remark 1. *The assumption $D_m = D_n$ is technically necessary for our global existence proof. It enables the critical step of combining m and n in the sum $\partial_t(m+n) - D\Delta(m+n)$, whose coercivity provides uniform L^∞-bounds. Unequal diffusion rates ($D_n > D_m$) are essential for Turing instabilities, and their analysis for global existence remains an open challenge beyond our current scope.*

2.2. Stability of the uniform steady state

We now investigate the steady-state solutions of system (1.4), which satisfy the following elliptic system with homogeneous Neumann boundary conditions:

$$\begin{cases} -D_m\Delta m = a - (b+1)m + \dfrac{cm^2}{1+m}n, & x \in \Omega, \\ -D_n\Delta n = bm - \dfrac{cm^2}{1+m}n, & x \in \Omega, \\ \dfrac{\partial m}{\partial \nu} = \dfrac{\partial n}{\partial \nu} = 0, & x \in \partial\Omega. \end{cases} \tag{2.1}$$

A direct computation reveals that the system admits a unique spatially homogeneous equilibrium

$$(m^*, n^*) = \left(a, \frac{b(1+a)}{ca}\right), \tag{2.2}$$

which corresponds to the uniform steady state under zero-flux boundary conditions. This equilibrium persists as the trivial solution to the steady-state system, representing the baseline chemical concentrations in the absence of spatial heterogeneities.

We now analyze the stability of the homogeneous steady state $\left(a, \frac{b(1+a)}{ca}\right)$. Let $\xi = (m, n)^T$, and the nonlinear reaction term $G(\xi)$ is explicitly defined as

$$G(\xi) = \left(a - (b+1)m + \frac{cm^2}{1+m}n,\ bm - \frac{cm^2}{1+m}n\right)^T,$$

which governs the autocatalytic dynamics. The linearized system of

$$\xi_t = \begin{pmatrix} D_m & 0 \\ 0 & D_n \end{pmatrix} \Delta\xi + G(\xi)$$

in $\Omega \times (0, \infty)$ can be expressed as

$$\xi_t = \begin{pmatrix} D_m & 0 \\ 0 & D_n \end{pmatrix} \Delta\xi + J_G(\xi_0)\xi,$$

where $J_G(\xi_0)$ denotes the Jacobian matrix of G evaluated at the steady state $\xi_0 = (a, \frac{b(1+a)}{ca})^T$.

Let $\{\lambda_k\}_{k=0}^{\infty}$ denote the eigenvalues of the negative Laplacian $-\Delta$ under homogeneous Neumann boundary conditions, ordered as

$$0 = \lambda_0 < \lambda_1 < \lambda_2 < \cdots < \lambda_k < \cdots,$$

with $\varsigma(\lambda_k)$ representing the multiplicity of λ_k. Define the phase space

$$X = \left\{\xi = (m, n)^T \in C^1(\overline{\Omega}) \times C^1(\overline{\Omega}) \ :\ \frac{\partial m}{\partial \nu} = \frac{\partial n}{\partial \nu} = 0 \text{ on } \partial\Omega\right\},$$

which admits the spectral decomposition:

$$X = \bigoplus_{k \geq 0} X_k, \tag{2.3}$$

where X_k is the eigenspace corresponding to λ_k.

Theorem 2. *Assume the inequality*

$$ca^2 > b - a - 1 \tag{2.4}$$

holds. If the principal eigenvalue λ_1 of the Dirichlet operator satisfies

$$\lambda_1 > \frac{b - a - 1}{D_m(1+a)} - \frac{ca^2}{D_n(1+a)}, \tag{2.5}$$

then the homogeneous steady state $\xi_0 = \left(a, \frac{b(1+a)}{ca}\right)^T$ of system (1.4) is uniformly asymptotically stable.

Proof. Consider small perturbations $\tilde{\xi} = (\tilde{m}, \tilde{n})^T$ around ξ_0. The linearized system is derived as

$$\tilde{m}_t = D_m\Delta\tilde{m} - (b+1)\tilde{m} + \frac{b(2+a)}{1+a}\tilde{m} + \frac{ca^2}{1+a}\tilde{n}, \tilde{n}_t = D_n\Delta\tilde{n} + b\tilde{n} - \frac{ca^2}{1+a}\tilde{n} - \frac{b(2+a)}{1+a}\tilde{m}, \tag{2.6}$$

where the reaction terms are linearized at ξ_0. The Jacobian matrix $J(\xi_0)$ in the eigenfunction basis becomes

$$J(\xi_0) = \begin{pmatrix} D_m\Delta + \frac{b}{1+a} - 1 & \frac{ca^2}{1+a} \\ -\frac{b}{1+a} & D_n\Delta - \frac{ca^2}{1+a} \end{pmatrix}.$$

For Laplacian eigenvalues $\{\lambda_k\}_{k=0}^{\infty}$ $(0 = \lambda_0 < \lambda_1 < \cdots)$ under Neumann conditions, the characteristic matrix for mode k is

$$A_k = \begin{pmatrix} -D_m\lambda_k + \frac{b}{1+a} - 1 & \frac{ca^2}{1+a} \\ -\frac{b}{1+a} & -D_n\lambda_k - \frac{ca^2}{1+a} \end{pmatrix}.$$

The determinant and trace of A_k are

$$\begin{cases} \det(A_k) = \lambda_k\left[D_mD_n\lambda_k + D_m\dfrac{ca^2}{1+a} - D_n\left(\dfrac{b}{1+a} - 1\right)\right] + \dfrac{ca^2}{1+a}, \\ \mathrm{Tr}(A_k) = \dfrac{b}{1+a} - 1 - \dfrac{ca^2}{1+a} - (D_m + D_n)\lambda_k. \end{cases} \tag{2.7}$$

To ensure stability, two conditions must hold. One is the positivity of $\det(A_k)$, that is,

$$\det(A_k) = D_mD_n\lambda_k[\lambda_k + \frac{ca^2}{D_n(1+a)} - \frac{b-a-1}{D_m(1+a)}] + \frac{ca^2}{1+a} > 0.$$

Substituting $\lambda_k \geq \lambda_1 > \frac{b-a-1}{D_m(1+a)} - \frac{ca^2}{D_n(1+a)}$, it follows that $\det(A_k) > 0$ for all $k \geq 1$. In addition, it is obvious that $\det(A_0) > 0$ when $k = 0$.

The other condition to ensure stability is the negativity of $\mathrm{Tr}(A_k)$. If $ca^2 > b-a-1$, then the constant term $\frac{b}{1+a} - 1 - \frac{ca^2}{1+a}$ is negative. Combined with $-(D_m + D_n)\lambda_k < 0$, this ensures $\mathrm{Tr}(A_k) < 0$ for all $k \geq 0$.

To sum up, under the given inequality and eigenvalue condition, both $\det(A_k) > 0$ and $\mathrm{Tr}(A_k) < 0$ hold for all $k \geq 1$. By linear stability theory, ξ_0 is uniformly asymptotically stable. The proof is complete. □

While diffusion is typically associated with homogenization, a previous study demonstrated that differential diffusion rates between system components can destabilize a spatially homogeneous equilibrium, even when it is stable in the absence of diffusion [23]. This mechanism is termed turing instability. In the following, we discuss this phenomenon for system (1.4).

Theorem 3. *Assume $ca^2 > b - a - 1 > 0$, and there exist critical diffusion coefficients $\widetilde{D}_m, \widetilde{D}_n > 0$ such that for $0 < D_m < \widetilde{D}_m$ and $D_n > \widetilde{D}_n$, the homogeneous steady state $\xi_0 = \left(a, \frac{b(1+a)}{ca}\right)^T$ is locally asymptotically stable for the non-diffusive system*

$$\frac{dm}{dt} = a - (b+1)m + \frac{cm^2}{1+m}n, \qquad \frac{dn}{dt} = bm - \frac{cm^2}{1+m}n, \tag{2.8}$$

while it is unstable for the diffusive system (1.4), indicating the onset of Turing bifurcation.

Proof. When diffusion is absent ($D_m = D_n = 0$), the Jacobian matrix $J_G(\xi_0)$ at ξ_0 is

$$J_G(\xi_0) = \begin{pmatrix} \frac{b}{1+a} - 1 & \frac{ca^2}{1+a} \\ -\frac{b}{1+a} & -\frac{ca^2}{1+a} \end{pmatrix}.$$

The trace and determinant are

$$\mathrm{Tr}(J_G) = \frac{b}{1+a} - 1 - \frac{ca^2}{1+a}, \quad \det(J_G) = \frac{ca^2}{1+a}\left(1 - \frac{b}{1+a}\right).$$

Given $ca^2 > b - a - 1 > 0$, we have $\mathrm{Tr}(J_G) < 0$ and $\det(J_G) > 0$. By linear stability theory, ξ_0 is asymptotically stable in the non-diffusive system (2.8).

For the diffusive system (1.4), we know from the proof of Theorem 2, the determinant of the characteristic matrix A_k for the k-th Laplacian eigenvalue is

$$\det(A_k) = \lambda_k \left[D_m D_n \lambda_k + D_m \frac{ca^2}{1+a} - D_n \left(\frac{b}{1+a} - 1 \right) \right] + \frac{ca^2}{1+a}.$$

Then we have

$$\lim_{D_m \to 0} \det(A_1) \leqslant \frac{1}{1+a} \left(ca^2 - \lambda_1 D_n (b - a - 1) \right).$$

For sufficiently small $\widetilde{D}_m$ and sufficiently large $\widetilde{D}_n$, we have $\det(A_1) < 0$ as $D_m < \widetilde{D}_m$ and $D_n > \widetilde{D}_n$. This implies A_1 has a positive eigenvalue, destabilizing ξ_0 in the presence of diffusion. Thus, Turing instability occurs. The proof is complete. □

Theorem 3 rigorously establishes that the interplay between reaction kinetics and diffusion disparities can destabilize the homogeneous equilibrium ξ_0, despite its stability in the non-diffusive system. The inequality $ca^2 > b - a - 1 > 0$ ensures that the system lies within a Turing space parameter regime where diffusion-driven pattern formation is feasible. The critical diffusion thresholds $\widetilde{D}_m$ and $\widetilde{D}_n$ delineate the transition from stability to instability, reflecting the competition between stabilizing reactions and destabilizing diffusion.

2.3. Non-constant solutions

2.3.1. Non-existence of non-constant solutions

In the following, we discuss the non-constant solutions of system (1.4). First, we present a lemma that will be used in the subsequent discussion. Readers can refer to [24].

Lemma 1. *Let $f \in C^1\left(\overline{\Omega} \times \mathbb{R}\right)$.*

(1) Suppose $\xi \in C^2(\Omega) \cap C^1(\overline{\Omega})$ satisfies

$$\Delta\xi + f(x, \xi) \geq 0 \quad \text{in } \Omega, \quad \frac{\partial \xi}{\partial \nu} \leq 0 \quad \text{on } \partial\Omega.$$

If ξ attains its maximum at $x_0 \in \overline{\Omega}$, then $f(x_0, \xi(x_0)) \geq 0$.

(2) Suppose $\xi \in C^2(\Omega) \cap C^1(\overline{\Omega})$ satisfies

$$\Delta\xi + f(x,\xi) \le 0 \quad \text{in } \Omega, \qquad \frac{\partial \xi}{\partial \nu} \ge 0 \quad \text{on } \partial\Omega.$$

If ξ attains its minimum at $x_0 \in \overline{\Omega}$, then $f(x_0, \xi(x_0)) \le 0$.

Proposition 2. *For any solution $\xi = (m,n)^T$ of system (2.1), the following bounds hold in Ω:*

$$\frac{a}{b+1} \le m \le a + \frac{D_n b(a+b+1)}{D_m ca}, \tag{2.9}$$

$$\frac{b\left(1 + a + \frac{D_n b(a+b+1)}{D_m ca}\right)}{c\left(a + \frac{D_n b(a+b+1)}{D_m ca}\right)} \le n \le \frac{b(a+b+1)}{ca}. \tag{2.10}$$

Proof. Let $x_0 \in \overline{\Omega}$ be a minimum point of m. By Lemma 1, the reaction term satisfies

$$a - (b+1)m(x_0) + \frac{cm^2(x_0)}{1+m(x_0)} n(x_0) \le 0.$$

Since $\frac{cm^2(x_0)}{1+m(x_0)} > 0$ and $n(x_0) > 0$, we deduce

$$a - (b+1)m(x_0) \le 0 \implies m(x_0) \ge \frac{a}{b+1}.$$

Thus, $m \ge \frac{a}{b+1}$ in Ω.

At a maximum point $x_1 \in \overline{\Omega}$ of n, Lemma 1 yields

$$bm(x_1) - \frac{cm^2(x_1)}{1+m(x_1)} n(x_1) \ge 0 \implies n(x_1) \le \frac{b(1+m(x_1))}{cm(x_1)}.$$

Define $F(m) = \frac{b(1+m)}{cm}$, which is strictly decreasing ($F'(m) = -\frac{b}{cm^2} < 0$). At the minimal $m = \frac{a}{b+1}$, $F(m)$ attains its maximum

$$F\left(\frac{a}{b+1}\right) = \frac{b(a+b+1)}{ca}.$$

Hence, $n \le \frac{b(a+b+1)}{ca}$ in Ω.

Define the weighted sum $W = D_m m + D_n n$. Adding the equations of (2.1),

$$-D_m \Delta m - D_n \Delta n = a - m.$$

This simplifies to $-\Delta W = a - m$. At a maximum point $x_2 \in \overline{\Omega}$ of W, Lemma 1 implies $a - m(x_2) \le 0$, so $m(x_2) \ge a$. Combining with the upper bound for n,

$$W(x_2) = D_m m(x_2) + D_n n(x_2) \le D_m a + D_n \cdot \frac{b(a+b+1)}{ca}.$$

Thus,

$$m(x) \le \frac{1}{D_m} W(x) \le \frac{1}{D_m} W(x_2) \le a + \frac{D_n b(a+b+1)}{D_m ca}, \quad \forall x \in \Omega.$$

At a minimum point $x_3 \in \overline{\Omega}$ of n, Lemma 1 gives

$$bm(x_3) - \frac{cm^2(x_3)}{1+m(x_3)}n(x_3) \le 0 \implies n(x_3) \ge \frac{b(1+m(x_3))}{cm(x_3)}.$$

Since $F(m)$ is decreasing, substituting the upper bound $m \le a + \frac{D_n b(a+b+1)}{D_m ca}$ yields

$$n \ge \frac{b\left(1 + a + \frac{D_n b(a+b+1)}{D_m ca}\right)}{c\left(a + \frac{D_n b(a+b+1)}{D_m ca}\right)}.$$

The proof is complete. □

By employing standard elliptic regularity theory and applying the uniform bounds established in Proposition 2, we derive the following result.

Proposition 3. *Fix parameters $a, b, \overline{D}_m, \overline{D}_n > 0$. For any positive integer $k \ge 1$, there exists a constant $\tilde{C} = \tilde{C}(a, b, \overline{D}_m, \overline{D}_n, k, N, \Omega) > 0$, such that for all $D_m \ge \overline{D}_m$ and $0 < D_n \le \overline{D}_n$, any solution $\xi = (m, n)^T$ of system (2.1) satisfies*

$$\|m\|_{C^k(\overline{\Omega})} + \|n\|_{C^k(\overline{\Omega})} \le \tilde{C}.$$

In particular, all solutions $\xi = (m, n)^T$ belong to $C^\infty(\overline{\Omega}) \times C^\infty(\overline{\Omega})$.

Proof. By Proposition 2, there must exist a constant $\tilde{K}(a, b, \overline{D}_m, \overline{D}_n) > 0$ such that solution $\xi = (m, n)^T$ satisfies

$$\|m\|_{L^\infty(\Omega)} + \|n\|_{L^\infty(\Omega)} \le \tilde{K}(a, b, \overline{D}_m, \overline{D}_n).$$

The reaction terms $f_1 = a - (b+1)m + \frac{cm^2 n}{1+m}$ and $g_1 = bm - \frac{cm^2 n}{1+m}$ are smooth, so there exists a constant $\tilde{K}_1(\tilde{K}, a, b, c) > 0$ such that

$$\|f_1\|_{L^\infty} + \|g_1\|_{L^\infty} \le \tilde{K}_1(\tilde{K}, a, b, c).$$

Schauder estimates for the elliptic system $-\Delta m = D_m^{-1} f_1, -\Delta n = D_n^{-1} g_1$ with Neumann conditions imply $m, n \in C^{1,\alpha}(\overline{\Omega})$ for some $\alpha \in (0, 1)$.

Since $f_1, g_1 \in C^\infty$ and $m, n \in C^{1,\alpha}$, the composition implies $f_1(m, n), g_1(m, n) \in C^{1,\alpha}(\overline{\Omega})$. Reapplying Schauder estimates inductively yields

$$m, n \in C^{k,\alpha}(\overline{\Omega}), \quad \|m\|_{C^k} + \|n\|_{C^k} \le \tilde{C}(a, b, \overline{D}_m, \overline{D}_n, k, N, \Omega)$$

for any $k \ge 1$. The constant $\tilde{C}$ depends on $\tilde{K}_1$ and Schauder constants at each bootstrap step. By the embedding $\bigcap_k C^{k,\alpha} = C^\infty$, we conclude $m, n \in C^\infty(\overline{\Omega})$. The proof is complete. □

Proposition 4. *Fix $a, b, D_n > 0$, and let $\{\sigma_k\} \subset (0, \infty)$ be a sequence with $\sigma_k \to \infty$ as $k \to \infty$. If $(m_k, n_k)^T$ is a solution sequence of system (2.1) with $D_m = \sigma_k$, then as $k \to \infty$,*

$$(m_k, n_k) \to \left(a, \frac{b(1+a)}{ca}\right) \quad \text{in } C^2(\overline{\Omega}) \times C^2(\overline{\Omega}). \tag{2.11}$$

Proof. By Proposition 3, the sequence $\{m_k, n_k\}$ is bounded in $C^3(\overline{\Omega}) \times C^3(\overline{\Omega})$. Thus, there exists a subsequence (still denoted by $\{m_k, n_k\}$) converging to some (m_∞, n_∞) in $C^2(\overline{\Omega}) \times C^2(\overline{\Omega})$.

Dividing the m_k-equation by σ_k and taking $k \to \infty$, we obtain

$$\begin{cases} -\Delta m_\infty = 0 \quad \text{in } \Omega, \\ \dfrac{\partial m_\infty}{\partial \nu} = 0 \quad \text{on } \partial\Omega. \end{cases} \tag{2.12}$$

By the maximum principle for harmonic functions with Neumann conditions, $m_\infty \equiv$ constant. Combining this with the conservation law in the non-diffusive system (Theorem 3), we conclude $m_\infty \equiv a$.

The n_∞-equation reduces to

$$-D_n \Delta n_\infty = ab - \frac{ca^2}{1+a} n_\infty \quad \text{in } \Omega, \qquad \frac{\partial n_\infty}{\partial \nu} = 0 \quad \text{on } \partial\Omega. \tag{2.13}$$

Multiplying both sides by $ab - \frac{ca^2}{1+a} n_\infty$ and integrating over Ω, we obtain

$$-D_n \int_\Omega \left(ab - \frac{ca^2}{1+a} n_\infty \right) \Delta n_\infty \, dx = \int_\Omega \left(ab - \frac{ca^2}{1+a} n_\infty \right)^2 dx. \tag{2.14}$$

Applying Green's formula to the left-hand side, we get

$$-D_n \int_\Omega \left(ab - \frac{ca^2}{1+a} n_\infty \right) \Delta n_\infty \, dx = -D_n \cdot \frac{ca^2}{1+a} \int_\Omega |\nabla n_\infty|^2 dx. \tag{2.15}$$

Substituting back, we deduce

$$D_n \cdot \frac{ca^2}{1+a} \int_\Omega |\nabla n_\infty|^2 dx + \int_\Omega \left(ab - \frac{ca^2}{1+a} n_\infty \right)^2 dx = 0. \tag{2.16}$$

Both terms are non-negative, implying

$$ab - \frac{ca^2}{1+a} n_\infty \equiv 0 \quad \text{and} \quad \nabla n_\infty \equiv 0. \tag{2.17}$$

Hence, $n_\infty \equiv \frac{b(1+a)}{ca}$. The proof is complete. □

Theorem 4. *(1) Let $a, b, D_n > 0$ be fixed. There exists $\overline{D}_m = \overline{D}_m(a, b, D_n) > 0$ such that for all $D_m > \overline{D}_m$, system (2.1) admits no non-constant solutions.*
(2) Let $a, D_m, D_n > 0$ be fixed. There exists $B = B(a, D_m, D_n) > 0$ such that for all $0 < b < B$, system (2.1) admits no non-constant solutions.

Proof. We only need to prove conclusion (1), and the proof for conclusion (2) is similar.

Let $(m, n)^T$ be a steady-state solution of (2.1). Integrating both equations over Ω and summing, we obtain

$$\int_\Omega m(x) \, dx = a|\Omega|. \tag{2.18}$$

Define the function spaces

$$H_n^2(\Omega) = \left\{ l \in W^{2,2}(\Omega) \,:\, \frac{\partial l}{\partial \nu} = 0 \right\}, \quad L_0^2(\Omega) = \left\{ l \in L^2(\Omega) \,:\, \int_\Omega l = 0 \right\}. \tag{2.19}$$

Let $l = m - a$. By elliptic regularity and the integral constraint $\int_\Omega m(x)\,dx = a|\Omega|$, system (2.1) is equivalent to

$$\begin{cases} -D_m \Delta l = a - (b+1)(a+l) + \dfrac{c(a+l)^2}{1+a+l} n, & x \in \Omega, \\ -D_n \Delta n = b(a+l) - \dfrac{c(a+l)^2}{1+a+l} n, & x \in \Omega, \end{cases} \tag{2.20}$$

where $l \in H_n^2(\Omega) \cap L_0^2(\Omega)$ and $n \in H_n^2(\Omega)$.

Let $\epsilon = \frac{1}{D_m}$, and rewrite the system as

$$\begin{cases} -\Delta l = \epsilon \left[a - (b+1)(a+l) + \dfrac{c(a+l)^2}{1+a+l} n \right], \\ -D_n \Delta n = b(a+l) - \dfrac{c(a+l)^2}{1+a+l} n. \end{cases} \tag{2.21}$$

Define the nonlinear operator

$$P : \mathbb{R} \times \left(H_n^2(\Omega) \cap L_0^2(\Omega) \right) \times H_n^2(\Omega) \to L_0^2(\Omega) \times L^2(\Omega), \tag{2.22}$$

$$P(\epsilon, l, n) = \begin{pmatrix} \Delta l + \epsilon \left(a - (b+1)(a+l) + \dfrac{c(a+l)^2}{1+a+l} n \right) \\ D_n \Delta n + b(a+l) - \dfrac{c(a+l)^2}{1+a+l} n \end{pmatrix}, \tag{2.23}$$

and it is easy to know that solving (2.21) is equivalent to solving $P(\epsilon, l, n) = 0$.

Obviously, $(l, n)^T = \left(0, \frac{b(1+a)}{ca}\right)^T$ is the unique homogeneous solution to $P(0, l, n) = 0$. The Fréchet derivative of $P(\epsilon, l, n)$ at $\left(0, 0, \frac{b(1+a)}{ca}\right)$ is

$$J_{(l,n)} P\left(0, 0, \frac{b(1+a)}{ca}\right) = \begin{pmatrix} \Delta & 0 \\ -\frac{b}{1+a} & D_n \Delta - \frac{ca^2}{1+a} \end{pmatrix}. \tag{2.24}$$

This operator is invertible due to the ellipticity and spectral gap: The term $-\frac{ca^2}{1+a} < 0$ ensures the spectrum of $D_n \Delta - \frac{ca^2}{1+a}$ is strictly negative, and this property, combined with the triangular structure, implies invertibility under Neumann boundary conditions.

By the implicit function theorem, there exists $\epsilon_0 > 0$ and a neighborhood $U_r\left(0, \frac{b(1+a)}{ca}\right)$ in $\left(H_n^2(\Omega) \cap L_0^2(\Omega)\right) \times H_n^2(\Omega)$ such that for $\epsilon \in [0, \epsilon_0]$, the only solution to $P(\epsilon, l, n) = 0$ is $(l, n)^T = \left(0, \frac{b(1+a)}{ca}\right)^T$.

Let $\{D_{m_k}\} \subset (0, \infty)$ with $D_{m_k} \to \infty$, and let $(m_k, n_k)^T$ be a solution sequence of (2.1) with $D_m = D_{m_k}$. Define $l_k = m_k - a$. By Proposition 4,

$$(l_k, n_k) \to \left(0, \frac{b(1+a)}{ca}\right) \quad \text{in } C^2(\overline{\Omega}) \times C^2(\overline{\Omega}).$$

For sufficiently large k, $\left(\frac{1}{D_{m_k}}, l_k, n_k\right)$ lies in $[0, \epsilon_0] \times U_r$, forcing $(l_k, n_k) = \left(0, \frac{b(1+a)}{ca}\right)$. Thus, there must exist $\overline{D}_m = \overline{D}_m(a, b, D_n) > 0$ such that system (2.1) has no nonconstant solutions when $D_m > \overline{D}_m$. The proof is complete. □

From Theorem 4, we know that when the activator's diffusion rate D_m exceeds a threshold $\overline{D}_m$, rapid diffusion of the activator homogenizes its concentration across the domain, preventing localized self-amplification. While when b falls below a threshold B, the activator's self-enhancement is too weak to overcome diffusion, or the inhibitor's production is inadequate to establish long-range suppression.

2.3.2. Existence of non-constant solutions

Having rigorously established parameter regimes where nonconstant steady states are mathematically excluded, thereby describing critical constraints for spatial homogeneity, we now turn to the complementary question of existence. Specifically, we will identify conditions under which spatially heterogeneous solutions emerge in system (2.1).

Let $X_+ = \left\{\xi = (m, n)^T \in X : m, n > 0\right\}$. Consider the elliptic system

$$-\Delta\xi = Y(\xi), \quad \xi \in X_+, \tag{2.25}$$

where the nonlinear reaction term is defined as

$$Y(\xi) = \begin{pmatrix} \frac{1}{D_m}\left(a - (b+1)m + \frac{cm^2}{1+m}n\right) \\ \frac{1}{D_n}\left(bm - \frac{cm^2}{1+m}n\right) \end{pmatrix}. \tag{2.26}$$

The eigenvalues of the operator $I - \Delta$ are $1 - \lambda_k$. If $\lambda_k \neq 1$ for all k, then $I - \Delta$ is invertible. Let $(I - \Delta)^{-1}$ denote its inverse, a bounded linear operator.

The steady-state Eq (2.25) can be rewritten as

$$(I - \Delta)\xi = Y(\xi) + \xi \quad \Longleftrightarrow \quad \xi = (I - \Delta)^{-1}(Y(\xi) + \xi). \tag{2.27}$$

We define the nonlinear operator

$$L(\xi) = \xi - \left[(I - \Delta)^{-1}(Y(\xi) + \xi)\right] = 0, \quad \xi \in X_+. \tag{2.28}$$

The homogeneous steady state $\xi_0 = \left(a, \frac{b(1+a)}{ca}\right)^T$ satisfies $L(\xi_0) = 0$.

The Fréchet derivative of L at ξ_0 is

$$\nabla L(\xi_0) = I - (I - \Delta)^{-1}(I + C),$$

where $C = \nabla Y(\xi_0)$ is the Jacobian matrix

$$C = \begin{pmatrix} \frac{b - a - 1}{D_m(1+a)} & \frac{ca^2}{D_m(1+a)} \\ -\frac{b}{D_n(1+a)} & -\frac{ca^2}{D_n(1+a)} \end{pmatrix}.$$

The Leray-Schauder index of the operator L at the homogeneous steady state ξ_0 is defined as [25]

$$\text{index}(L, \xi_0) = (-1)^{\gamma},$$

where γ denotes the algebraic count of negative eigenvalues of the Fréchet derivative $\nabla L(\xi_0)$.

With the spectral decomposition (2.3), X_k represents an invariant subspace under $\nabla L(\xi_0)$. The Fréchet derivative $\nabla L(\xi_0)$ has a spectral decomposition linked to the Laplacian eigenvalues $\{\lambda_k\}_{k=0}^{\infty}$ with Neumann boundary conditions. Specifically, its eigenvalues κ satisfy that

$$\kappa \text{ is an eigenvalue of } \nabla L(\xi_0) \iff \kappa \text{ is an eigenvalue of } (\lambda_k + 1)^{-1}(\lambda_k I - C).$$

Consequently, $\nabla L(\xi_0)$ is invertible if and only if the matrix $\lambda_k I - C$ is invertible for all $k \geq 0$.

Define the determinant function

$$Z(a, b, D_m, D_n, \lambda) = \det(\lambda I - C). \tag{2.29}$$

Explicitly

$$Z(a, b, D_m, D_n, \lambda) = \lambda^2 - \left[\frac{b - a - 1}{D_m(1 + a)} - \frac{ca^2}{D_n(1 + a)}\right]\lambda + \frac{ca^2}{D_m D_n(1 + a)}.$$

Then $\lambda_k I - C$ is invertible if and only if $Z(\lambda_k) \neq 0$. The algebraic count γ of negative eigenvalues of $\nabla L(\xi_0)$ is

$$\gamma = \sum_{\substack{k\geq 0 \\ Z(a,b,D_m,D_n,\lambda_k)<0}} \varsigma(\lambda_k), \tag{2.30}$$

where $\varsigma(\lambda_k)$ is the multiplicity of λ_k.

Through calculation, we can see that if the inequality

$$\frac{b}{1 + a} > \left(1 + \sqrt{\frac{D_m}{D_n} \cdot \frac{ca^2}{1 + a}}\right)^2$$

holds, then $Z = 0$ has two positive roots

$$\lambda^{\pm} = \frac{1}{2}\varrho(a, b, D_m, D_n) \pm \sqrt{\varrho(a, b, D_m, D_n)^2 - 4\frac{ca^2}{D_m D_n(1 + a)}},$$

where $\varrho(a, b, D_m, D_n) = \frac{b-a-1}{D_m(1+a)} - \frac{ca^2}{D_n(1+a)}$.

Similar to the method used in [17, 26], we can get the following result.

Theorem 5. *Assume the inequality*

$$\frac{b}{1 + a} > \left(1 + \sqrt{\frac{D_m}{D_n} \cdot \frac{ca^2}{1 + a}}\right)^2 \tag{2.31}$$

holds. Furthermore, suppose there exists $i > j \geq 0$ such that: (1) $\lambda_j < \lambda^- < \lambda_{j+1}$ and $\lambda_i < \lambda^+ < \lambda_{i+1}$, and (2) the total multiplicity $\sum_{k=j+1}^{i} \varsigma(\lambda_k)$ is odd, and system (2.1) admits at least one non-constant solution.

Proof. The proof employs topological degree theory. The eigenvalue interval $(\lambda_j, \lambda_i]$ in condition (1) defines the summation range $k = j+1$ to i for $\gamma = \sum_{k=j+1}^{i} \varsigma(\lambda_k)$ in $\text{index}(L, \xi_0) = (-1)^\gamma$. Condition (2) then guarantees γ is odd, yielding $\text{index}(L, \xi_0) = -1$.

By Theorem 4, for $D_m > \overline{D}_m$, system (2.1) possesses no non-constant solutions, and the determinant function $Z(a, b, D_m, D_n, \lambda) > 0$ for all $\lambda \geq 0$.

In addition, from Proposition 3, there exist constants $C_1, C_2 > 0$, depending on a, b, D_m, D_n, such that for any $D_m \geq \overline{D}_m$, all solutions $\xi = (m, n)^T$ of (2.1) satisfy

$$C_1 < m, n < C_2 \quad \text{in } \overline{\Omega}.$$

Define the admissible set

$$\mathcal{K} = \left\{(\xi, \eta) \in C(\overline{\Omega}) \times C(\overline{\Omega}) : C_1 < m, n < C_2 \text{ in } \overline{\Omega}\right\}.$$

Construct a homotopy map $\mathcal{P} : [0, 1] \times \mathcal{K} \to C(\overline{\Omega}) \times C(\overline{\Omega})$ as

$$\mathcal{P}(t, \xi) = (-\Delta + I)^{-1} \begin{pmatrix} m + \left(\frac{1-t}{\overline{D}_m} + \frac{t}{D_m}\right)\left(a - (b+1)m + \frac{cm^2}{1+m}n\right) \\ n + \frac{1}{D_n}\left(bm - \frac{cm^2}{1+m}n\right) \end{pmatrix}. \tag{2.32}$$

Obviously, the non-constant solution of (2.1) corresponds to the fixed point of $\mathcal{P}(t, \cdot)$ within $\mathcal{K}$. By Proposition 3 and the definition of $\mathcal{K}$, $\mathcal{P}(t, \cdot)$ has no fixed points on $\partial\mathcal{K}$ for $t \in [0, 1]$. Thus, the Leray-Schauder degree $\deg(I - \mathcal{P}(t, \cdot), \mathcal{K}, 0)$ is well-defined. If system (2.1) has no non-constant solutions, then by (2.30) we deduce

$$\deg(I - \mathcal{P}(1, \cdot), \mathcal{K}, 0) = \text{index}(L, \xi_0) = (-1)^{\sum_{k=j+1}^{i} \varsigma(\lambda_k)} = -1,$$

where $\xi_0 = \left(a, \frac{b(1+a)}{ca}\right)^T$. However, by the homotopy invariance of the topological degree,

$$\deg(I - \mathcal{P}(1, \cdot), \mathcal{K}, 0) = \deg(I - \mathcal{P}(0, \cdot), \mathcal{K}, 0).$$

For $\mathcal{P}(0, \cdot)$, the homogeneous equilibrium ξ_0 is its only fixed point. Since $Z(a, b, D_m, D_n, \lambda) > 0$ for all $\lambda \geq 0$, we derive

$$\deg(I - \mathcal{P}(0, \cdot), \mathcal{K}, 0) = \text{index}(I - \mathcal{P}(0, \cdot), \xi_0) = 1.$$

This contradiction implies the existence of at least one non-constant solution for system (2.1). The proof is complete. □

3. Numerical simulations

This section presents numerical simulations to validate the theoretical results established in the preceding analysis. All simulations were conducted on a one-dimensional spatial domain $\Omega = (0, 1)$ subject to homogeneous Neumann boundary conditions ($\partial m/\partial x = \partial n/\partial x = 0$ at $x = 0, 1$), representing a closed reaction-diffusion system with conserved total mass.

First, we select model parameters $a = 1$, $b = 3$, $c = 2$, $D_m = 0.1$, and $D_n = 0.1$, which satisfy the stability criteria $ca^2 = 2 > b - a - 1 = 1$ and $\lambda_1 > 0 > \frac{b-a-1}{D_m(1+a)} - \frac{ca^2}{D_n(1+a)} = -5$. Initial

conditions are prescribed as spatially perturbed versions of the homogeneous steady state $\xi_0 = (1, 3)^T$, incorporating sinusoidal disturbances of ±10% amplitude while maintaining compatibility with the Neumann boundary constraints. Figure 1 demonstrates rapid temporal convergence of $m(x, t)$ and $n(x, t)$ to the uniform equilibrium ξ_0 within $t = 15$ time units, accompanied by complete spatial homogenization. This behavior corroborates Theorem 2, confirming that the stability threshold $\lambda_1 > \frac{b-a-1}{D_m(1+a)} - \frac{ca^2}{D_n(1+a)}$ accurately predicts the system's asymptotic behavior under perturbations. From a biological perspective, these results underscore the inherent stability of the reactant equilibrium in a fully mixed chemical reaction system, where diffusive transport and reaction kinetics collaborate to restore spatial homogeneity despite initial heterogeneous disturbances.

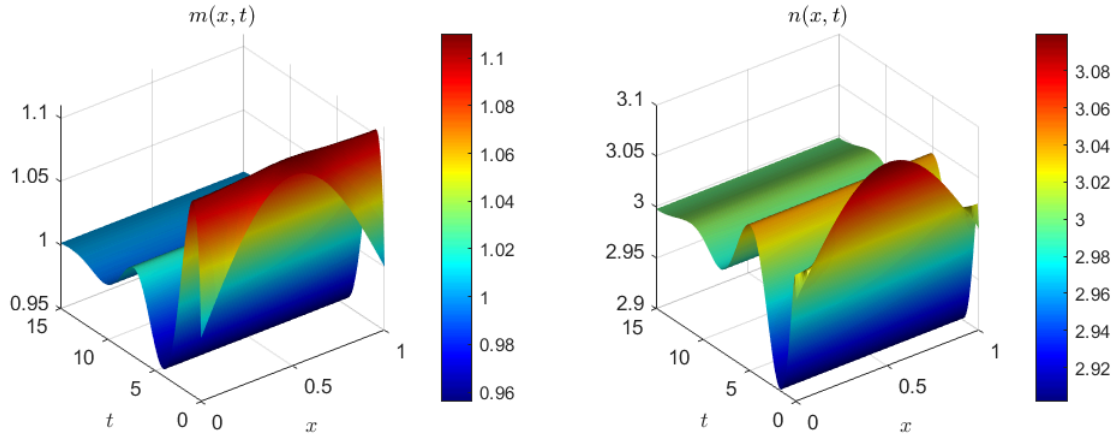

Figure 1. The uniform asymptotical stability of the homogeneous steady state ξ_0 of system (1.4).

To examine pattern formation dynamics, we maintain the reaction parameters $a = 1$, $b = 3$, and $c = 2$ (satisfying $ca^2 = 2 > b - a - 1 = 1$) while adjusting the diffusion coefficients to $D_m = 0.01$ and $D_n = 1.0$. For comparison, Figure 2(a) displays the solution curves of the corresponding non-diffusive system, confirming global asymptotic stability of the homogeneous steady state $\xi_0 = (1, 3)^T$ and validating the local stability analysis presented in Theorem 3. In contrast, the diffusive system with spatially perturbed initial conditions ($m_0(x) = 1 + 0.1\sin(\pi x) + 0.05\sin(2\pi x) + 0.02\cos(3\pi x)$ and $n_0(x)$ with similar perturbations) exhibits markedly different behavior. As shown in Figure 2(b), pronounced spatial heterogeneity emerges and persists in both $m(x, t)$ and $n(x, t)$ by $t = 100$. Quantitative analysis reveals substantial spatial variation with coefficients of variation $CV_m = 0.76$ and $CV_n = 0.027$, where $m(x)$ varies dramatically from approximately 0.4 to 2.7 across the spatial domain while $n(x)$ exhibits a complementary gradient from 2.65 to 2.85. These significant deviations from the homogeneous equilibrium provide conclusive evidence of diffusion-driven instability characteristics of turing pattern formation.

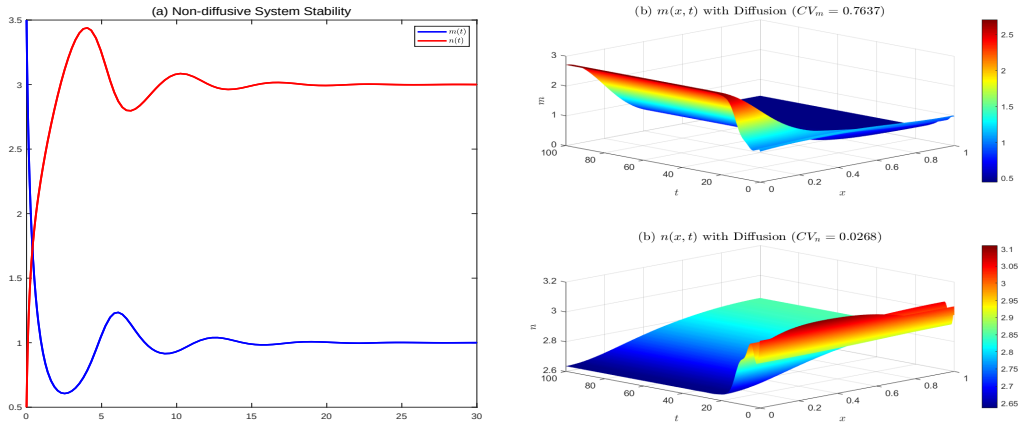

Figure 2. Diffusion-driven instability. (a) The stability of the homogeneous steady state for the non-diffusive system; (b) spatial heterogeneity of the diffusive system.

Subsequently, we conduct systematic numerical investigations across multiple parameter regimes to validate Theorem 4, elucidating the intricate relationship between model coefficients and spatial pattern emergence. With $b = 3$ held constant, we examine the effect of varying the diffusion coefficient D_m on pattern suppression. At $D_m = 0.5$, modest deviations from the homogeneous steady state $\xi_0 = (1, 3)^T$ are observed, quantified by standard deviations $\text{std}_m = 0.0052$ and $\text{std}_n = 0.0240$, indicating weak spatial fluctuations. Upon increasing D_m to 10, both concentration profiles $m(x)$ and $n(x)$ approach the uniform state with negligible spatial variations ($\text{std}_m \approx 0$, $\text{std}_n \approx 0$), as illustrated in Figure 3(a). This behavior provides empirical confirmation of the theoretical prediction regarding the existence of a critical threshold $\overline{D}_m$ above which non-constant solutions are eliminated.

Conversely, with $D_m = 0.1$ fixed, we investigate the influence of the parameter b on pattern formation intensity. At $b = 50$, pronounced spatial variations emerge ($\text{std}_m = 0.7986$, $\text{std}_n = 1.9048$), reflecting strong Turing-type instability. As b decreases to 3, these spatial deviations are substantially reduced ($\text{std}_m = 0.0081$, $\text{std}_n = 0.0083$), as demonstrated in Figure 3(b). This trend aligns quantitatively with the theoretical framework of Theorem 4, which predicts the existence of a positive threshold B below which pattern formation is inhibited.

Finally, we present comprehensive numerical validation of Theorem 5 concerning the existence conditions for non-constant solutions. The parameter configuration $a = 1.0$, $b = 20.0$, $c = 2.0$, $D_m = 0.05$, and $D_n = 0.02$ satisfies both requisite conditions of the theorem. First, the fundamental inequality $\frac{b}{1+a} > \left(1 + \sqrt{\frac{D_m}{D_n}} \cdot \frac{ca^2}{1+a}\right)^2$ is numerically verified, yielding $10.000 > 6.662$. Second, the spectral interval $[\lambda^-, \lambda^+] = [2.5, 22.5]$ contains precisely one eigenvalue ($\lambda_1 \approx 9.87$) of the Neumann Laplacian operator on $\Omega = (0, 1)$, thereby satisfying the odd multiplicity criterion.

The computed steady-state solutions presented in Figure 4(a) exhibit substantial spatial heterogeneity, characterized by non-trivial coefficients of variation ($cv_m = 0.0366$, $cv_n = 0.0155$). These significant deviations from the homogeneous equilibrium $\xi_0 = (1, 20)^T$ provide conclusive evidence for the existence of stable non-constant solutions. The corresponding eigenvalue analysis in Figure 4(b) illustrates the spectral distribution of the Laplacian operator, where the critical bounds λ^- and λ^+ delineate the destabilizing spectral region. The presence of a single eigenvalue λ_1 within

this interval triggers a bifurcation mechanism, in complete accordance with the odd multiplicity requirement specified in Theorem 5.

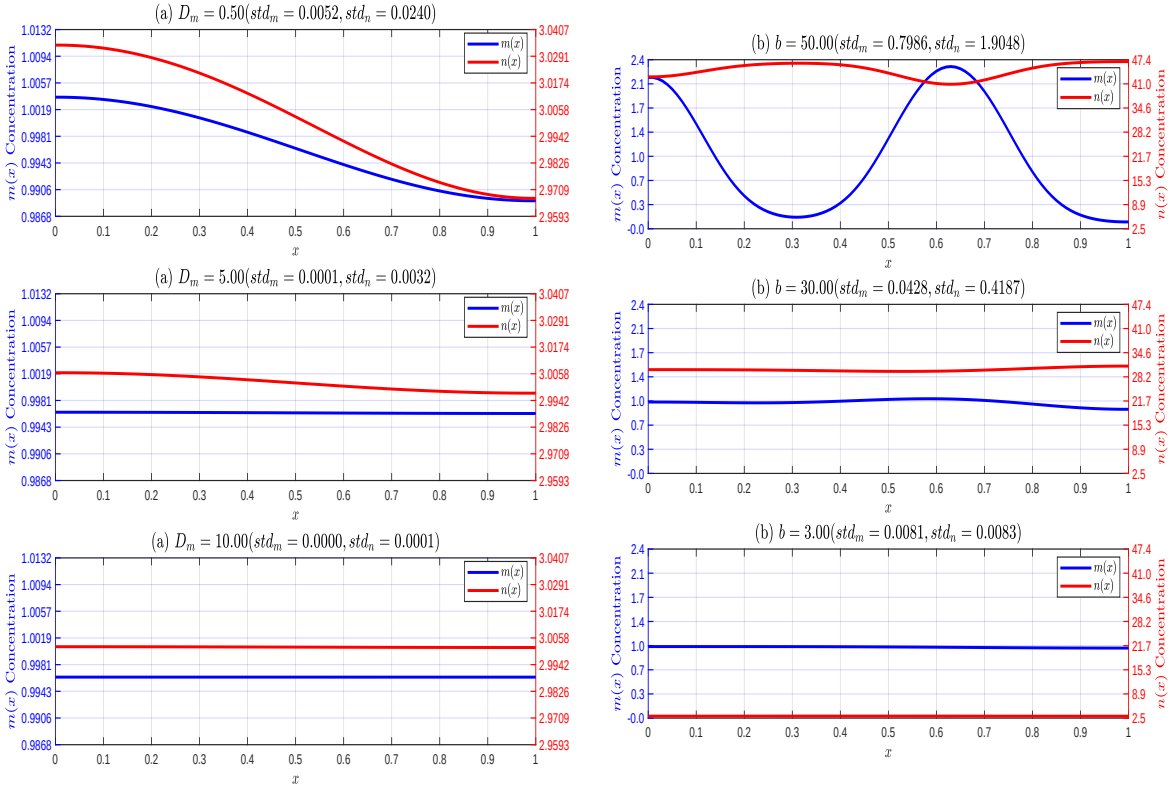

Figure 3. Diffusion-driven instability. (a) Impact of parameter D_m on the spatial pattern of system (2.1); (b) impact of parameter b on the spatial pattern of system (2.1).

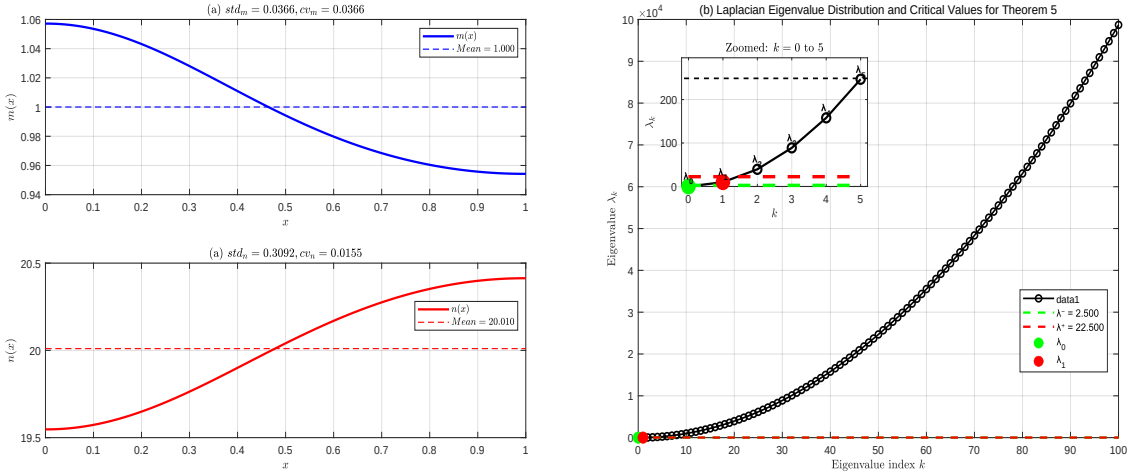

Figure 4. Pattern formation analysis: (a) Spatial distribution of steady-state solutions $m(x)$ and $n(x)$ exhibiting spatial heterogeneity; (b) eigenvalue spectrum showing the destabilizing eigenvalue λ_1 in the critical spectral region $[\lambda^-, \lambda^+]$.

4. Conclusions

This work presents a comprehensive theoretical and numerical analysis of pattern formation in a Brusselator reaction-diffusion model with nonlinear inhibition. Through mathematical analysis and numerical simulations, we have established key criteria that determine when spatial patterns emerge, remain stable, or disappear in this system.

Our theoretical analysis shows that the interaction between diffusion and nonlinear reactions creates complex dynamics that lead to pattern formation. Specifically, we found that the stability of uniform steady states depends on the balance between diffusion effects (which tend to create uniformity) and reaction mechanisms (which can create instability), as described by the critical conditions in Theorems 2–5. The explicit stability criteria we derived allow us to predict when spatial patterns will form or be eliminated.

From a theoretical chemistry viewpoint, our results demonstrate how self-organized spatial patterns emerge in the Brusselator reaction-diffusion system. We revealed that Turing pattern formation is critically dependent on both the ratio of diffusion coefficients and nonlinear reaction kinetics, indicating that homogeneous chemical systems can spontaneously generate ordered spatial structures despite initially uniform conditions.

The numerical simulations strongly support our theoretical predictions across different parameter ranges. The agreement between theoretical criteria and computational results confirms that our mathematical framework can reliably predict system behavior. Additionally, our systematic parameter studies clearly show transitions between stable uniform states and complex spatial patterns, confirming the threshold behavior predicted by theory.

Author contributions

Shouzong Liu: Conceptualization; supervision; methodology; Yaxin Niu: Writing–original draft preparation; Peiyang Chai: Writing–review and editing. All authors have read and approved the final version of the manuscript for publication.

Use of Generative-AI tools declaration

The authors declare that they have not used Artificial Intelligence (AI) tools in the creation of this article.

Acknowledgments

This work is supported by the National Natural Science Foundation of China (12271466), Scientific and Technological Key Projects of Henan Province (242102110374), Natural Science Foundation of Henan Province (252300420346), and Nanhu Scholars Program for Young Scholars of XYNU.

Conflict of interest

The authors declare that they have no competing interests.

References

1. I. R. Epstein, J. A. Pojman, *An introduction to nonlinear chemical dynamics: Oscillations, waves, patterns, and chaos*, New York: Oxford Academic, 1998. https://doi.org/10.1093/oso/9780195096705.001.0001
2. M. C. Cross, P. C. Hohenberg, Pattern formation outside of equilibrium, *Rev. Mod. Phys.*, **65** (1993), 851–1112. https://doi.org/10.1103/RevModPhys.65.851
3. P. Gray, S. K. Scott, Autocatalytic reactions in the isothermal, continuous stirred tank reactor: Isolas and other forms of multistability, *Chem. Eng. Sci.*, **38** (1983), 29–43. https://doi.org/10.1016/0009-2509(83)80132-8
4. I. Prigogine, R. Lefever, Symmetry breaking instabilities in dissipative systems, II, *J. Chem. Phys.*, **48** (1968), 1695–1700. https://doi.org/10.1063/1.1668896
5. A. M. Alqahtani, Numerical simulation to study the pattern formation of reaction-diffusion Brusselator model arising in triple collision and enzymatic, *J. Math. Chem.*, **56** (2018), 1543–1566. https://doi.org/10.1007/s10910-018-0859-8
6. R. M. Jena, S. Chakraverty, H. Rezazadeh, D. D. Ganji, On the solution of time-fractional dynamical model of Brusselator reaction-diffusion system arising in chemical reactions, *Math. Method. Appl. Sci.*, **43** (2020), 3903–3913. https://doi.org/10.1002/mma.6141
7. S. Zhao, P. Yu, W. Jiang, H. Wang, A new mechanism revealed by cross-diffusion-driven instability and double-Hopf bifurcation in the Brusselator system, *J. Nonlinear Sci.*, **35** (2025), 1–40. https://doi.org/10.1007/s00332-024-10107-6
8. P. Gray, S. K. Scott, J. H. Merkin, The Brusselator model of oscillatory reactions, *J. Chem. Soc. Farandy Trans. 1*, **84** (1988), 993–1012. https://doi.org/10.1039/F19888400993
9. J. J. Tyson, *What everyone should know about the Belousov-Zhabotinsky reaction*, In: Frontiers in Mathematical Biology, Lecture Notes in Biomathematics, Berlin: Springer, **100** (1994), 569–587. https://doi.org/10.1007/978-3-642-50124-1_33
10. B. Li, G. Guo, *Diffusion-driven instability and Hopf bifurcation in spatial homogeneous Brusselator model*, In: Advances in Future Computer and Control Systems, Advances in Intelligent and Soft Computing, Berlin: Springer, **160** (2012), 249–255. https://doi.org/10.1007/978-3-642-29390-0_41
11. Y. Lv, Z. Liu, Turing-Hopf bifurcation analysis and normal form of a diffusive Brusselator model with gene expression time delay, *Chaos Soliton. Fract.*, **152** (2021), 111478. https://doi.org/10.1016/j.chaos.2021.111478
12. M. Chen, R. Wu, B. Liu, L. Chen, Turing-Turing and Turing-Hopf bifurcations in a general diffusive Brusselator model, *J. Appl. Math. Mec.*, **103** (2023), e201900111. https://doi.org/10.1002/zamm.201900111
13. H. Liu, B. Ge, Spatial Turing patterns of periodic solutions for the Brusselator system with cross-diffusion-like coupling, *Int. J. Bifurcat. Chaos*, **33** (2023), 2350148. https://doi.org/10.1142/S0218127423501481
14. M. Liao, Q. R. Wang, Stability and bifurcation analysis in a diffusive Brusselator-type system, *Int. J. Bifurcat. Chaos*, **26** (2016), 1650119. https://doi.org/10.1142/S0218127416501194

15. D. V. Kriukov, J. Huskens, A. S. Y. Wong, Exploring the programmability of autocatalytic chemical reaction networks, *Nat. Commun.*, **15** (2024), 8289. https://doi.org/10.1038/s41467-024-52649-z
16. X. Zhu, M. Huang, H. Bao, X. Zhang, Mechanistic insights into nonlinear effects in copper-catalyzed asymmetric esterification, *Nat. Commun.*, **16** (2025), 2183. https://doi.org/10.1038/s41467-025-57380-x
17. M. Ghergu, V. Radulescu, Turing patterns in general reaction-diffusion systems of Brusselator type, *Commun. Contemp. Math.*, **12** (2010), 661–679. https://doi.org/10.1142/S0219199710003968
18. L. Kong, C. Zhu, Diffusion-driven codimension-2 Turing-Hopf bifurcation in the general Brusselator model, *Math. Method. Appl. Sci.*, **44** (2021), 11456–11468. https://doi.org/10.1002/mma.7504
19. H. Y. Alfifi, Feedback control for a diffusive and delayed Brusselator model: Semi-analytical solutions, *Symmetry*, **13** (2021), 725. https://doi.org/10.3390/sym13040725
20. M. Winkler, A three-dimensional Keller-Segel-Navier-Stokes system with logistic source: Global weak solutions and asymptotic stabilization, *J. Funct. Anal.*, **276** (2019), 1339–1401. https://doi.org/10.1016/j.jfa.2018.12.009
21. J. Zheng, Y. Ke, Eventual smoothness and stabilization in a three-dimensional Keller-Segel-Navier-Stokes system modeling coral fertilization, *J. Differ. Equations*, **328** (2022), 228–260. https://doi.org/10.1016/j.jde.2022.04.042
22. J. Zheng, P. Zhang, X. Liu, Global existence and boundedness for an N-dimensional parabolic-elliptic chemotaxis-fluid system with indirect pursuit-evasion, *J. Differ. Equations*, **367** (2023), 199–228. https://doi.org/10.1016/j.jde.2023.04.042
23. A. Turing, The chemical basis of morphogenesis, *Philos. T. Roy. Soc. B*, **237** (1952), 37–72. https://doi.org/10.1098/rstb.1952.0012
24. Y. Lou, W. M. Ni, Diffusion vs cross-diffusion: An elliptic approach, *J. Differ. Equations*, **154** (1999), 157–190. https://doi.org/10.1006/jdeq.1998.3559
25. L. Nirenberg, *Topics in nonlinear functional analysis*, New York: New York University-Courant Institute of Mathematical Sciences, **6** (2001). https://doi.org/10.1090/cln/006
26. R. Peng, J. Shi, M. Wang, On stationary patterns of a reaction-diffusion model with autocatalysis and saturation law, *Nonlinearity*, **21** (2008), 1471–1488. https://doi.org/10.1088/0951-7715/21/7/006

AIMS Press